

# Twin electroweak bubble nucleation and gravitational wave under the $S_3$ symmetry of two-Higgs-doublet model

Vo Quoc Phong<sup>a,b\*</sup> and Nguyen Xuan Vinh<sup>a,b†</sup>

<sup>a</sup>*Department of Theoretical Physics, University of Science, Ho Chi Minh City 700000, Vietnam*

<sup>b</sup>*Vietnam National University, Ho Chi Minh City 700000, Vietnam*

Phan Hong Khiem<sup>c,d‡</sup>

<sup>c</sup>*Institute of Fundamental and Applied Sciences,*

*Duy Tan University, Ho Chi Minh City 700000, Vietnam*

<sup>d</sup>*Faculty of Natural Sciences, Duy Tan University, Da Nang City 50000, Vietnam*

Sphaleron electroweak phase transition (EWPT) is calculated in two phase transition stages, thereby showing that the twin (or double) bubble nucleation structure of the phase transition and gravitational wave is in the investigation area of future detectors. With  $v^2 = v_1^2 + v_2^2$  ( $v_1$  and  $v_2$  are two vacuum average values (VEV)), the parameter  $\tan \beta = v_2/v_1$ , is the ratio between two VEVs although it does not affect the strength of EWPT but affect the sphaleron energy. However, it only causes this energy to increase slightly. As  $a = v^2/v_2^2$  increases, the maximum difference of sphaleron energy in one stage is about 6.15 TeV.  $a$  affects the expansion of bubbles during two phase transitions. The more  $a$  increases, the more the expansion of two bubbles is at the same time. This ratio does not greatly affect the sphaleron energy but has an impact on gravitational waves. The larger the masses of the charged Higgs particles are, the greater the gravitational wave energy density ( $\Omega h^2$ ) is. When the frequency is in the range  $0 - 1.2$  mHz,  $\Omega h^2$  will have a maximum value in the range  $10^{-12} - 10^{-11}$  for all values of  $a$  so this can be detected in the future.

PACS numbers: 11.15.Ex, 12.60.Fr, 98.80.Cq

---

\* vqphong@hcmus.edu.vn

† vinhnguyen.mxt@gmail.com

‡ phanhongkhiem@duytan.edu.vn

Keywords: Spontaneous breaking of gauge symmetries, Extensions of electroweak Higgs sector, Particle-theory models (Early Universe)

## CONTENTS

I. INTRODUCTION	2
II. Controlling EWPT in The 2HDM with $S_3$ symmetry	5
A. The Higgs potential	5
B. The temperature effective Higgs potential and cotronling EWPT	7
III. Sphalerons and Gravitational waves in the 2HDM- $S_3$	13
A. Sphaleron	13
B. Gravitational waves	15
IV. CONCLUSION AND OUTLOOKS	20
ACKNOWLEDGMENTS	21
A. Table of data	22
References	25

## I. INTRODUCTION

Particle physics today not only studies each individual problem in depth but also combines it with Cosmology and Astronomy. The baryon asymmetry is a problem of intersection among those fields. The possible causes of this problem are summarized and presented quite extensively. Indeed, for Higgs 125 GeV, Standard Model (SM) has only a second order electroweak phase transition when the mass of Higgs is greater than 75 GeV [1–6]. Therefore, SM should be extended (for example, Refs. [7–53]). There are 3 main branches: the first is due to the existence of exotic particles (beyond the standard model (SM)); the second is because of parameters or interactions in SM changing at a electroweak transition temperature [7–45, 47–53]; the third be having more than 4 dimensions of spacetime [54].

Except for the Leptogenesis scenario, the more familiar one for the baryon asymmetry is Baryogenesis. The center condition is a first order electroweak phase transition [55], is needed to sufficiently maintain a thermal imbalance at a critical temperature during the mass generation of elementary particles. This condition down to calculating the high-temperature effective Higgs potential and investigating the electroweak phase transition (EWPT).

Two scenarios are commonly seen when analyzing the structure of EWPT process: the single-stage scenario as in Refs. [56–60], most theories under this scenario are models that modify SM; and mixed or separated multi-phase scenarios [7, 23, 61, 62], via models have group structures different from SM.

Currently there are three methods to survey the effective potential of EWPT process. The first method: The effective potential  $V_{eff}(v)$  which is a function of  $v$  (VEV), written jointly for two VEVs and  $v^2 = v_1^2 + v_2^2$ . The second one in Refs. [63, 64]: the effective potential is a function of two VEVs but EWPT is still one phase as SM. The third method is ours, in Ref.[65]: the effective potential into two separate parts [ $V_{eff} = V_{eff}(v_1) + V_{eff}(v_2)$ ] and examining two discrete stages.

The two Higgs model with  $S_3$  symmetry (2HDM- $S_3$ ) [66], an extended version of 2HDM, has been studied by us in terms of strigers for a first order electroweak phase transitions [65]. Other roles of  $S_3$  symmetry in the quark sector or the Yukawa couplings, are discussed in Refs. [67–70].

The above center condition was solved in the two-Higgs-doublet model with  $S_3$  symmetry. When adding the  $S_3$  symmetry to 2HDM, it makes the path of EWPT process discrete. This decoherence is expressed by two discretization stages corresponding to two VEVs. Typically, the first phase goes with  $v_2$ , the second phase goes with  $v_1$ .

$$\begin{aligned}
& 2\text{HDM-}S_3 \\
& \Downarrow \text{breaking } v_2 \\
& \Downarrow \text{breaking } v_1 \\
& U(1)_Q
\end{aligned}$$

The  $S_3$  symmetry acts as the one to simplify the parameters of Higgs potential and can make the EWPT process discrete. But it does not play the dominant role in terms of particle interaction dynamics in 2HDM. Therefore, the value domains of  $\tan \beta$  drawn from different data in 2HDM are still valid in 2HDM- $S_3$ . These remarks are like the following conclusions:

- According to Ref. [64, 67, 68, 71, 72], when calculating decay channels and combining LHC data,  $1 < \tan \beta < 17$ . Cases of  $\tan \beta$  less than one do not exist. The masses of heavy particles are more than 190 GeV [63, 73, 74].
- On the other hand, the independent gauge of EWPT (specifically the effective potential and the phase transition strength) [37–39, 59, 75]. The daisy loops are not the main cause of EWPT but reduces the strength of EWPT [76]. Therefore, when investigating around the electroweak phase transition temperature region, for simplicity we can ignore their contributions.
- In Refs. [77–80], the strong first order EWPT in 2HDM with the condition, the hierarchy of mass,  $m_{H^\pm} < m_H < m_A$  and  $1 < \tan \beta < 10$ .
- The results in Refs. [81, 82] confirm that the masses of additional Higgs bosons are typically 300 – 400 GeV for a first order EWPT.
- Furthermore, in Ref. [64, 83–86] there are many scenarios among the additional Higgs bosons were studied in the EWPT problem, specifically  $m_{H^\pm} = m_A$  or  $m_H = m_{H^\pm}$ .

The above conclusions lead to an instruction for surveying 2HDM- $S_3$  also with a parameter region,  $1 \sim \tan \beta < 17$  and the masses of additional bosons must be larger than 200 GeV. Our result in Ref.[65] agrees with the above conclusions and the results in Ref. [64, 87–89], which concludes that  $\tan \beta$  is not a meaningful parameter in 2HDM. This is also the motivation for us to fully study the Baryogenesis scenario in 2HDM- $S_3$ .

The main results of Ref.[65] are outlined as follows. The ratio parameter  $\tan \beta$  does not cause the dynamics of phase transition and the effective potential should be written as two components, each corresponding to a VEV. However,  $\tan \beta$  determines the value range of additional particles. The  $S_3$  symmetry acts as a "boundary" between the two electroweak phase transitions.

To complete the Baryogenesis scenario in 2HDM- $S_3$  and continue the results of Ref.[65], this paper presents the calculations of sphaleron and gravitational wave. Sphaleron is a process associated with the  $B$  violation, so calculating and testing its rules to more firmly confirm the solution of baryon asymmetry problem in this model. Gravitational waves (GW) produced in the EWPT are almost a accompanying problem that can be connected to experimental data of current detectors.

The sphaleron energy functional is currently calculated in two different ways (the ansatz with scale-free parameters [90] and the smooth one [91, 92]) but both require numerical solutions, which we summarize in Ref.[56]. Similarly, the key parameters and calculation of gravitational wave energy density are also summarized in Ref.[61].

In addition, the effect of  $S_3$  symmetry should be further evaluated even though dynamically the one has no impact. The difference among sphaleron energies and gravitational wave energy densities at the two phase transitions are considered. These bandgaps are sketched as phenomenologically the effects of  $S_3$  symmetry.

The paper has the following structure. Except for the Introduction (Sec. I) and the Conclusion and Outlooks (Sec. IV), Appendix A and Sec. II discusses the control of first order electroweak phase transition problem. This is a summary of the results in Ref.[65] and an analysis of the phase transition strength in values of  $a$  to further confirm the independence of  $S$  according to  $a$ . More importantly, we show how to control an first order electroweak phase transition. In Sec. III we derive the sphaleron energy functional and the gravitational wave energy density which undergoes important parameters. Then we solve them and compare the results with existing data or evaluate them.

## II. CONTROLLING EWPT IN THE 2HDM WITH $S_3$ SYMMETRY

The search for a first order electroweak phase transition is essential, it outlines a possible path to the matter-antimatter asymmetry problem. This has been done and evaluated in Ref.[65]. In this section, the conditions for a first order EWPT will be comprehensively evaluated.

### A. The Higgs potential

The generic scalar potential of 2HDM- $S_3$  [66, 93] in the complex representation, has a simpler form that contains 5 real parameters:

$$V_{\text{Higgs}}^{2\text{HDM}\otimes S_3} \equiv V(\phi_1, \phi_2) = \mu_1^2(\phi_2\phi_2^\dagger + \phi_1\phi_1^\dagger) + \frac{1}{2}l_1(\phi_2\phi_2^\dagger + \phi_1\phi_1^\dagger)^2 + \frac{1}{2}l_2(\phi_2\phi_2^\dagger - \phi_1\phi_1^\dagger)^2 \\ + l_3(\phi_1^\dagger\cdot\phi_2)(\phi_2^\dagger\cdot\phi_1) - \mu_2^2\left(\phi_1^\dagger\cdot\phi_2 + \phi_2^\dagger\cdot\phi_1\right) + H.C. \quad (1)$$

The above potential is obtained from adding  $S_3$  symmetry and the  $S_3$  soft violating

potential to the initial position of 2HDM. The process of calculation and reduction to the above potential is the resetting of scalar fields and parameters presented in Refs.[66, 93]. Eq. (1) has mixed components between  $\phi_1$  and  $\phi_2$  but is much simpler than the original 2HDM potential.

The fields  $\phi_1$  and  $\phi_2$  have the following VEVs:

$$\langle\phi_1\rangle_0 = \frac{1}{\sqrt{2}} \begin{pmatrix} 0 \\ v_1 \end{pmatrix}, \langle\phi_2\rangle_0 = \frac{1}{\sqrt{2}} \begin{pmatrix} 0 \\ v_2 \end{pmatrix}. \quad (2)$$

For a model with more than one VEV, there is usually a scaling parameter among the VEVs that are included to investigate phenomenological problems. In the model of interest, a very familiar parameter is introduced manually,

$$\tan \beta = \frac{s_\beta}{c_\beta} = \frac{v_2}{v_1}, \quad (3)$$

where  $s_\beta \equiv \sin \beta$ ,  $c_\beta \equiv \cos \beta$ .  $\beta$  is the mixing angle between the charged Higgs and pseudoscalar particle. The value of  $\tan \beta$  is summarized in the introduction section.

When calculating the EWPT problem, the Higgs and gauge boson sector have the strongest contributions. After diagonalizing Eq.(1) and the gauge field sector [65], the masses of Higgs fields are like Eq.(4).

$$\begin{aligned} m_{H^\pm}^2 &= -l_2 v^2, m_A^2 = -\frac{1}{2}(2l_2 - l_3)v^2, \\ m_H^2 &= \frac{v^2}{4} \left[ 2l_1 + l_3 + \sqrt{16l_1 l_2 (c_\beta^2 - s_\beta^2)^2 - 8l_2 l_3 + l_3^2 - 4l_1 l_3 (c_\beta^4 - 6c_\beta^2 s_\beta^2 + s_\beta^4)} \right] = \frac{f_H}{4} v^2, \\ m_h^2 &= \frac{v^2}{4} \left[ 2l_1 + l_3 - \sqrt{16l_1 l_2 (c_\beta^2 - s_\beta^2)^2 - 8l_2 l_3 + l_3^2 - 4l_1 l_3 (c_\beta^4 - 6c_\beta^2 s_\beta^2 + s_\beta^4)} \right] = \frac{f_h}{4} v^2. \end{aligned} \quad (4)$$

The masses of  $H^\pm$  and  $A$  have no mixing between the two VEVs, this is not possible in the 2HDM model. Similarly, the gauge particles also do not have this mixing. However, we cannot eliminate this mixing for  $H$  and  $h$  either, so we are forced to approximate  $f_H$  and  $f_h$ . The mass spectra of them can be derived by expanding the kinetic energy component of the higgs field. The mass spectra of all particles that contribute significantly to the EWPT process in Table I.

In this model  $v^2 = v_2^2 + v_1^2$ , we put  $v^2 = a.v_2^2$ . Therefore, the masses of particles in terms of  $a$  are given in Table II.

Particles	$m(v_0)$ [GeV]	$m^2(v_1, v_2)$	$m^2(v_1)$	$m^2(v_2)$	$n$
$W^\pm$	80.442	$\frac{g^2 v^2}{4}$	$\frac{g^2 v_1^2}{4}$	$\frac{g^2 v_2^2}{4}$	6
$Z$	91.18	$(g^2 + g'^2) \frac{v^2}{4}$	$(g^2 + g'^2) \frac{v_1^2}{4}$	$(g^2 + g'^2) \frac{v_2^2}{4}$	3
$h$	125	$\frac{1}{4} f_h v^2$	$\frac{1}{4} f_h v_1^2$	$\frac{1}{4} f_h v_2^2$	1
$H$	—	$\frac{1}{4} f_H v^2$	$\frac{1}{4} f_H v_1^2$	$\frac{1}{4} f_H v_2^2$	1
$A$	—	$-\frac{1}{2} (2l_2 - l_3) v^2$	$-\frac{1}{2} (2l_2 - l_3) v_1^2$	$-\frac{1}{2} (2l_2 - l_3) v_2^2$	1
$H^\pm$	—	$-l_2 v^2$	$-l_2 v_1^2$	$-l_2 v_2^2$	2
$t$	173.1	$f_t^2 v^2$	$f_t^2 v_1^2$	$f_t^2 v_2^2$	-12

TABLE I: Squared mass of the gauge bosons and scalar bosons in 2HDM- $S_3$ ; whereas mass of the  $W^\pm$ ,  $Z$  and  $t$  is the same as the one in SM;  $v^2 = v_1^2 + v_2^2$ ;  $v_0 = 246$  GeV.

Particles	$m^2(v_1, v_2)$	$m^2(v_2)$	$m^2(v_1)$
$m_{W^\pm}^2$	$\frac{g^2 v^2}{4}$	$m_{W^\pm}^2/a$	$m_{W^\pm}^2(v_2).(a-1)$
$m_Z^2$	$(g^2 + g'^2) \frac{v^2}{4}$	$m_Z^2/a$	$m_Z^2(v_2).(a-1)$
$m_h^2$	$\frac{1}{4} f_h v^2$	$m_h^2/a$	$m_h^2(v_2).(a-1)$
$m_H^2$	$\frac{1}{4} f_H v^2$	$m_H^2/a$	$m_H^2(v_2).(a-1)$
$m_A^2$	$-\frac{1}{2} (2l_2 - l_3) v^2$	$m_A^2/a$	$m_A^2(v_2).(a-1)$
$m_{H^\pm}^2$	$-l_2 v^2$	$m_{H^\pm}^2/a$	$m_{H^\pm}^2(v_2).(a-1)$
$m_t^2$	$f_t^2 v^2$	$m_t^2/a$	$m_t^2(v_2).(a-1)$

TABLE II: Squared mass of the gauge and scalar bosons in 2HDM- $S_3$ .

## B. The temperature effective Higgs potential and cotronling EWPT

We see that there is a problem in examining the phase transition. Why is  $v_1$  different from  $v_2$  (meaning the vacuum breaking process of the two Higgs fields is different) that we examine them together? We examine the electroweak phase transition with two stages, because of the following two reasons: the first, as the above sections pointed out, in 2HDM- $S_3$ , the masses of particles ( $H$  and  $h$ ) can be changed such that there are no mixing terms between  $v_1$  and  $v_2$ . This approximation is similar to the way of examining a phase transition where  $v_1$  and  $v_2$  are both brought to the variable  $v$ . The second, we do not ignore the mixing

of VEVs in the mass components, we only approximate them. Therefore, with  $v_1$  different from  $v_2$ , this model has two stages of phase transition and assume  $v_1 < v_2$ , which means  $1 < a < 2$  or  $1 < \tan \beta$ . So the approximate effective potential for this model is

$$V_{eff}^{S_3} \approx V_{eff}^{S_3}(v_1) + V_{eff}^{S_3}(v_2). \quad (5)$$

The mixing components between  $v_1$  and  $v_2$  have been absorbed into  $V_{eff}^{S_3}(v_1)$  and  $V_{eff}^{S_3}(v_2)$  when using  $\tan \beta$  or  $a$ , as shown in Table II. Hence in Eq.5, although the effective potentials are separated, the mixing components are still present in them. In addition, although the electroweak phase transition is investigated with two phases, these phases may interact with each other through the mixing components in the mass components of the particles. This will be investigated further in this paper.

With the above formula for the potential, the phase transition strength does not depend on  $a$ . This has been proven in Ref.[65]. The high-temperature effective potential when considering daisy loops is rewritten as follows,

$$V_{eff}(\phi, T) = \lambda(T)\phi^4 + D(T^2 - T_0^2)\phi^2 - \frac{T}{12\pi} \sum_{h,W,Z,H,H^\pm,A} g_i \left[ \frac{m_i^2 \phi^2}{v_{b0}^2} + \Pi_i(T) \right]^{\frac{3}{2}}. \quad (6)$$

where,  $b = 1, 2$  then  $v_{10}, v_{20}$  are  $v_1, v_2$  at  $T = 0$  respectively and

$$\begin{aligned} \lambda(T) &= \frac{m_h^2 + m_H^2}{8v_{b0}^2} + \frac{1}{64\pi^2 v_{b0}^4} \sum_{h,W,Z,H,H^\pm,A,t} g_i m_i^4 \ln \left( \frac{A_i T^2}{m_i^2} \right), \\ D &= \frac{m_h^2 + 6m_W^2 + 3m_Z^2 + m_H^2 + 2m_{H^\pm}^2 + m_A^2 + 6m_t^2}{24v_{b0}^2}, \\ T_0^2 &= \frac{1}{D} \left[ \frac{m_h^2 + m_H^2}{4} - \sum_{h,W,Z,H,H^\pm,A,t} \frac{g_i m_i^4}{32\pi^2 v_{b0}^2} \right], \\ \Pi_W(T) &= \frac{22}{3} \frac{m_W^2}{v_{b0}^2} T^2, \quad \Pi_Z(T) = \frac{22}{3} \frac{(m_Z^2 - m_W^2)}{v_{b0}^2} T^2, \\ \Pi_h(T) &= \frac{m_h^2 + 2m_W^2 + m_Z^2 + 2m_t^2}{4v_{b0}^2} T^2, \\ \Pi_A(T) &\sim \frac{m_A^2}{v_{b0}^2} T^2, \quad \Pi_{H^\pm}(T) \sim \frac{m_{H^\pm}^2}{v_{b0}^2} T^2, \quad \Pi_H(T) \sim \frac{m_H^2}{v_{b0}^2} T^2. \end{aligned} \quad (7)$$

In Eq.7,  $\ln A_i = 3.907$  or  $\ln A_i = 1.135$  for bosons or fermions.  $\Pi_W(T)$ ,  $\Pi_Z(T)$ ,  $\Pi_A(T)$ ,  $\Pi_{H^\pm}(T)$ ,  $\Pi_H(T)$  are functions that characterize the daisy loop contributions. The daisy loops of charged Higgs ( $H^\pm$ ), neutral Higgs ( $H$ ) and  $A$  are omitted because the transition temperatures less than 200 GeV, the contribution of these loops is negligible. This has been



clearly demonstrated in the articles [65, 102]. Also with another method of calculating the thermal phase transition, in Ref.[103] without daisy loop components.

In addition, the calculation of the effective potential with the daisy loops of the heavy Higgs particles in the temperature effective potential is necessary for completeness of the problem. However, we need to see that the main driving force of these particles is the trigger for the EWPT process. Therefore, adding these loops may complicate the main calculation because their contributions are negligible in the context of the EWPT calculation.

From many conclusions, we propose a way to investigate or control the Higgs potential to have a first order phase transition or  $S = \frac{v_c}{T_c} > 1$  ( $v_c$  and  $T_c$  are VEV and critical temperature respectively): the first is to build the high temperature effective potential. The second is to select the investigation variable, usually the masses of new particles. Finally, survey in the absence of daisy loops. Specify the range of values for variables to have  $S > 1$ . If the masses of new particles are greater than 200 GeV, there are no need to use additional daisy loops.

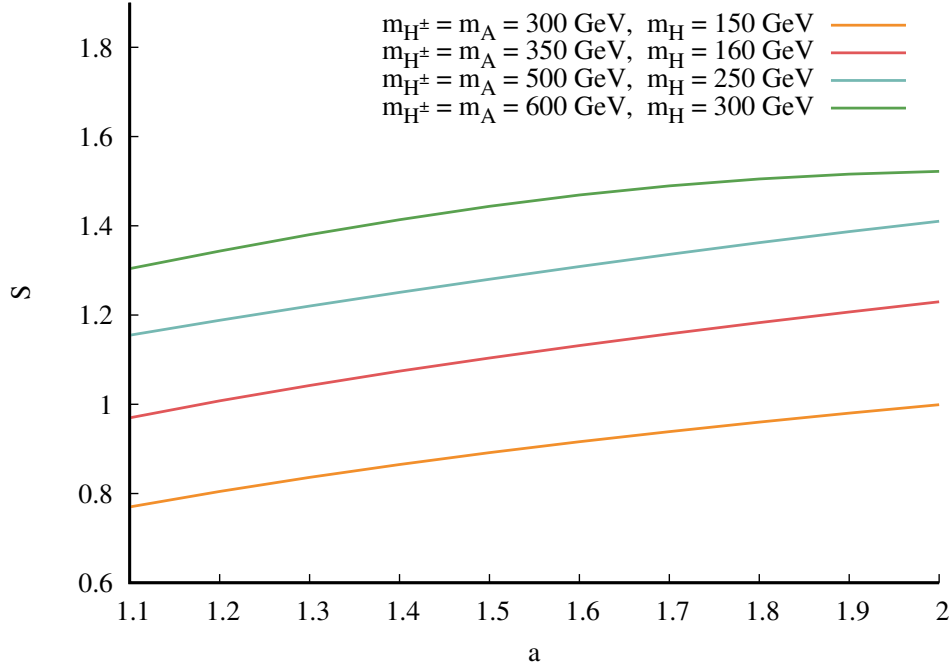


FIG. 1: The strength of EWPT is a function of  $a$ . The masses of particles are in GeV.  $m_{H^\pm}, m_A$  and  $m_H$  in the figure are just  $m_{H^\pm}(v_2), m_A(v_2)$  and  $m_H(v_2)$ .

In Fig. 1, the strength  $S$  almost does not change with  $a$ , for different mass cases. This is another way to confirm the results of previous article (in Ref.[65]). Also in Fig.1, the lines are not absolutely parallel to the  $a$  axis (the slopes are very small). This means that

$S$  still depends on  $a$ , because the  $\Pi$  functions which are the contributions of daisy loops, still depend on  $a$  but are negligible. Through such analysis, also following many conclusions from other authors, it is once again fully confirmed that the contribution of daisy loops in the vicinity of critical temperature ( $T_c \sim 100 - 150$  GeV) is negligible.

With different mass pairs, the values of phase transition strength do not vary too much. These masses are arbitrary but falls within the range of values drawn from other studies. Not any mass pair of two particles gives a first order EWPT. The three parameters including  $a$  and the two mass parameters are bound together. This is one of the conditions that can be used as a reference for the mass range of new particles. Thus the search for a first order electroweak phase transition depends on the masses of particles and even  $a$  (when considering daisy loops).

As in Ref.[65], the value of  $a$  is in the range 1 to 2.  $a$  (or  $\tan \beta$ ) is the parameter that is entered by hand, in the electroweak phase transition problem, although it has no role in influencing the strength of phase transition, but physically, it characterizes the distance between two phase transitions.

There are two ways to control a first order phase transition: the first, choose the masses of the particles (which must also be large enough), then control  $a$  to find  $S > 1$  as in this article (although the dependence on  $a$  is quite small when taking into account daisy loops); the second, which is the way done in Ref. [65]. For models with multiple phase transitions, we should do both of these to cross-check the results.

According to Fig. 2, the two potential functions corresponding to  $v_2$  and  $v_1$  get closer to each other as  $a$  increases. With the uniform convergence of second minima (i.e. always less than 246 GeV), the two effective potentials are always similar to each other. Although Fig.2 only corresponds to one mass pair, it is quite general, other mass pairs are presented in Appendix A.

Replacing the investigation in terms of  $\tan \beta$  with  $a$  actually gives an advantage in sketching the evolution of two components in the effective potential. Mathematically, the value domain of  $\tan \beta$  is an open one (i.e. there is no upper bound). But when examined in terms of  $a$ , the value domain of  $a$  is closed, it lies between 1 and 2. This change is like a mapping of  $\tan \beta$  into  $a$ . In summary, finding a first order electroweak phase transition with an effective potential pair in 2HDM- $S_3$  is mathematically and physically feasible.

a	$v_c$ [GeV]	$T_c$ [GeV]	$S$	$E_{sph,b}^T$ [GeV]	$\alpha$	$\frac{\beta}{H_*}$	$\Omega h^2(f_{peak}) \times 10^{-14}$
1.1	$v_2=154.618$	159.443	0.969736	7841.47	0.017436	22.1311	1.82991
	$v_1=48.8945$	50.4204	0.969735	2479.69	0.0174359	22.1311	1.8299
1.2	$v_2=153.951$	152.784	1.00764	7588.49	0.019334	22.3506	2.70965
	$v_1=68.8489$	68.3271	1.00764	3393.67	0.019334	22.3506	2.70965
1.3	$v_2=153.12$	146.913	1.04225	7365.48	0.0211846	22.5607	3.82934
	$v_1=83.8672$	80.4677	1.04225	4034.24	0.0211846	22.5607	3.82934
1.4	$v_2=152.188$	141.682	1.07415	7166.8	0.02299	22.7626	5.21179
	$v_1=96.2521$	89.6077	1.07415	4532.68	0.02299	22.7626	5.21179
1.5	$v_2=151.2$	136.979	1.10382	6988.23	0.0247537	22.9576	6.87871
	$v_1=106.914$	96.8587	1.10382	4941.43	0.0247537	22.9576	6.87871
1.6	$v_2=150.187$	132.717	1.13164	6826.53	0.0264803	23.1465	8.85171
	$v_1=116.335$	102.802	1.13164	5287.81	0.0264803	23.1465	8.85171
1.7	$v_2=149.173$	128.83	1.15791	6679.16	0.0281746	23.3302	11.1534
	$v_1=124.807$	107.787	1.15791	5588.19	0.0281746	23.3302	11.1534
1.8	$v_2=148.175$	125.264	1.1829	6544.11	0.0298422	23.5091	13.8084
	$v_1=132.531$	112.039	1.1829	5853.23	0.0298422	23.5091	13.8084
1.9	$v_2=147.203$	121.977	1.20681	6419.72	0.0314887	23.6838	16.8449
	$v_1=139.649$	115.717	1.20681	6090.28	0.0314887	23.6838	16.8449
2	$v_2=146.268$	118.934	1.22982	6304.68	0.03312	23.8544	20.2955
	$v_1=146.268$	118.934	1.22982	6304.68	0.03312	23.8544	20.2955

TABLE III: Results in case  $m_{H^\pm}(v_2) = m_A(v_2) = 350$  GeV,  $m_H(v_2) = 160$  GeV.

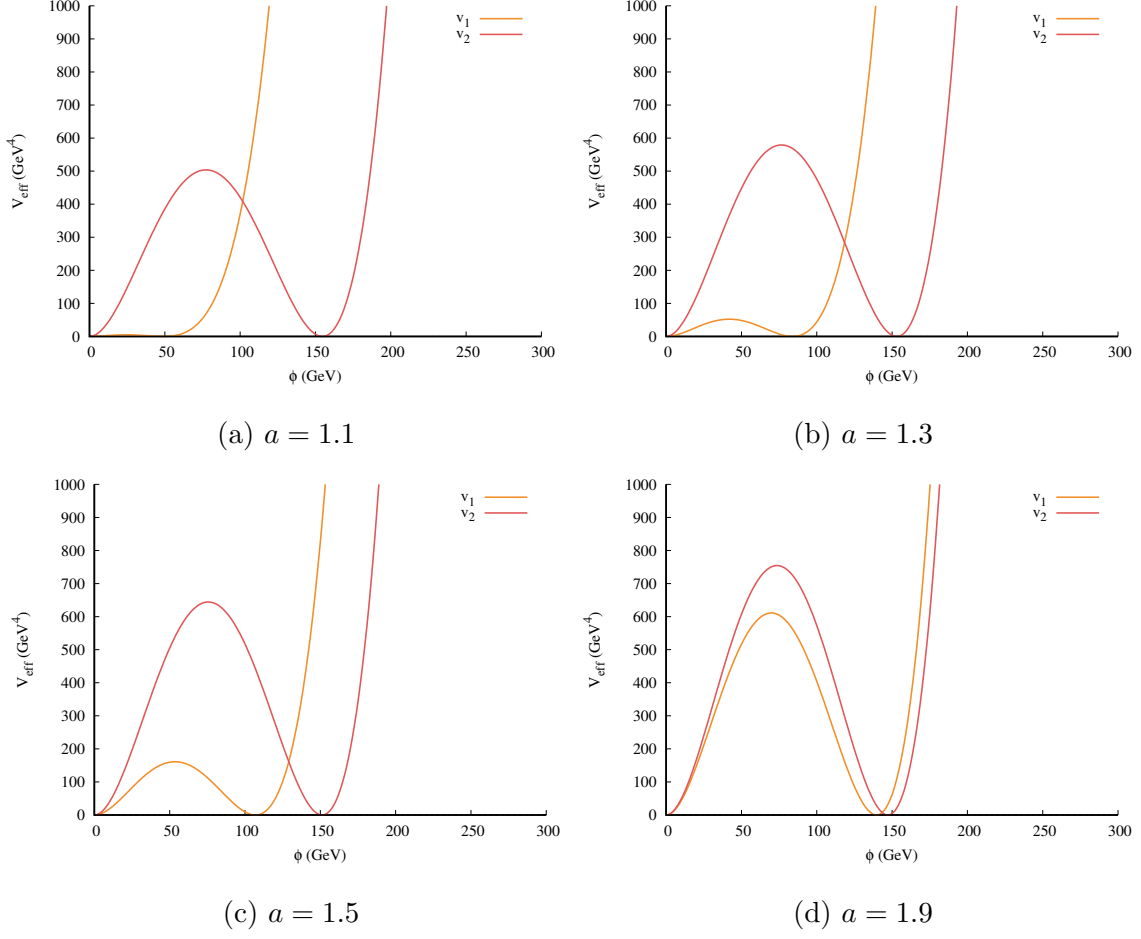


FIG. 2: The effective potential  $V_{eff}$  at  $T = T_c$ .  $m_{H^\pm}(v_2) = m_A(v_2) = 350$  GeV,  $m_H(v_2) = 160$  GeV. The red line corresponds to  $V_{eff}(v_2)$ . The orange line corresponds to  $V_{eff}(v_1)$ .

In Fig.2, the non-zero minimum of effective potential corresponding to  $v_2$  is always larger than that of  $v_1$ . The yellow lines in Fig.2 approach the red lines as  $a$  increases or the two phase transitions get closer together. When  $a = 2$ , the two potential functions coincide, but then the electroweak phase transition is the simultaneous phase transition of two VEVs. This corresponds to the existence of two scalar Higgs fields in this model. It is interesting to note that these two scalar fields are partly involved in both phase transitions. No one scalar particle is involved in only one phase transition. The nature of this problem is that the higgs potential contains up to two Higgs doublets and is a general mixture of these two doublets. Furthermore, in Table III, for a given value of  $a$ ,  $S$  of the two EWPT stages are the same. This confirms the results in Ref.[65]. However, to find the maximum value of  $S$  which is often not very precise, the method in Ref.[65] gives better results.

### III. SPHALERONS AND GRAVITATIONAL WAVES IN THE 2HDM- $S_3$

The 2HDM model with the  $S_3$  symmetry shows a "twin bubble nucleation or double bubble nucleation". The first possible demonstration of this is that the masses of particles depends on the two VEVs. Two bubbles can form at the same time or one after the other. The following numerical analysis will clarify that.

#### A. Sphaleron

The sphaleron energy functional consists of three components: the contribution of gauge fields, Higgs kinetic energy and effective potential.

$$E_{sph} = \int dx^3 \left[ \frac{1}{4} W_{ij}^a W_{ij}^a + (D_i \phi)^\dagger (D_i \phi) + V_{eff} \right]. \quad (8)$$

The contributions of exotic Higgs bosons ( $H^\pm$ ,  $A$  and  $H$ ) can be ignored. However, they still contribute to the effective potential components. The static field approximation (ie.,  $W_0^a = 0$ ) has been assumed and sphaleron has a spherically symmetric form [91]:

$$\begin{cases} \phi(r) = \frac{v_0}{\sqrt{2}} h(r) i n_a \sigma \begin{pmatrix} 0 \\ 1 \end{pmatrix}, \\ W_i^a(r) = \frac{2}{g} \epsilon^{aij} n_j \frac{f(r)}{r}, \end{cases} \quad (9)$$

where  $n_i \equiv \frac{x^i}{r}$  and  $r$  is the radial coordinate in the spherical coordinates. The functions  $h(r), f(r)$  are profile functions, which characterize bubbles.

The Sphaleron energy functional at temperature  $T$  is written as follows

$$E_{sph}^T = \frac{4\pi v_0}{g} \int_0^\infty d\xi \left[ 4 \left( \frac{df}{\xi} \right)^2 + \frac{8f^2(1-f)^2}{\xi^2} + \frac{\xi^2}{2} \left( \frac{dh}{\xi} \right)^2 + h^2(1-f)^2 + \frac{\xi^2}{g^2 v_0^4} V_{eff}(h, T) \right], \quad (10)$$

where  $g^2 = \frac{G_F 8m_W^2}{\sqrt{2}}$ ;  $G_F = 1.166 \times 10^{-5} \text{ GeV}^{-2}$ ;  $m_W = 80.39 \text{ GeV}$ ,  $\xi \equiv g v_0 r$ .

To make the above function converge in the process of solving, the last term is rewritten as a difference. Thus specifically for each stage will be

$$\begin{aligned} E_{sph,b}^T = \frac{4\pi v_{b0}}{g} \int_0^\infty d\xi \left[ 4 \left( \frac{df_b}{d\xi} \right)^2 + \frac{8}{\xi^2} f_b^2 (1-f_b)^2 + \frac{\xi^2}{2} \left( \frac{dh_b}{d\xi} \right)^2 + h_b^2 (1-f_b)^2 \right. \\ \left. + \frac{\xi^2}{g^2 v_{b0}^4} (V_{eff}(v_{c,b} h_b, T_{c,b}) - V_{eff}(v_{c,b}, T_{c,b})) \right]. \quad (11) \end{aligned}$$

Taking the variation of above function in terms of  $h$  and  $f$ , after minimizing the Sphaleron functional, the equations of motion are obtained,

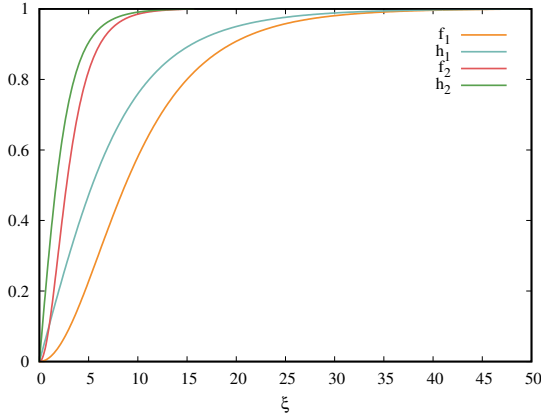
$$\frac{d^2 f_b}{d\xi^2} = \frac{2}{\xi^2} f_b(1 - f_b)(1 - 2f_b) - \frac{1}{4}(1 - f_b)h_b^2, \quad (12)$$

$$\frac{d^2 h_b}{d\xi^2} = \frac{-2}{\xi} \frac{dh_b}{d\xi} + \frac{2}{\xi^2} h_b(1 - f_b)^2 + \frac{1}{g^2 v_{b0}^4} \frac{\partial V_{eff}(v_{c,b} h_b, T_{c,b})}{\partial h_b}. \quad (13)$$

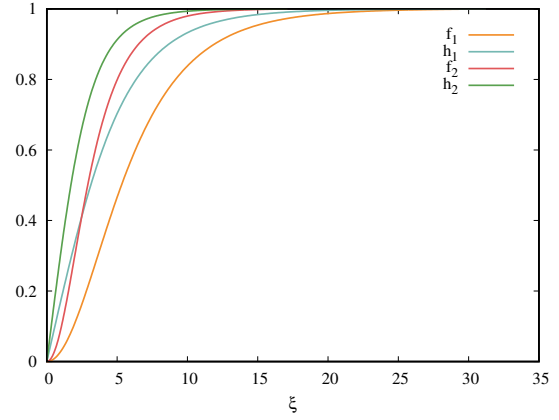
Here,  $h_b(\xi)$  and  $f_b(\xi)$  have boundary conditions,

$$\begin{cases} h_b(\xi \rightarrow 0) = f_b(\xi \rightarrow 0) = 0, \\ h_b(\xi \rightarrow \infty) = f_b(\xi \rightarrow \infty) = 1. \end{cases} \quad (14)$$

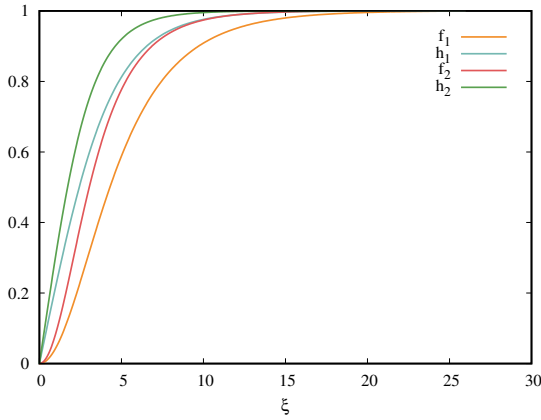
Note that in the above equations, the run index  $b = 1, 2$  is the phase transition of  $v_{1,2}$ , respectively. From Eqs. (12,13,14), the numerical solutions are obtained as Fig.3.



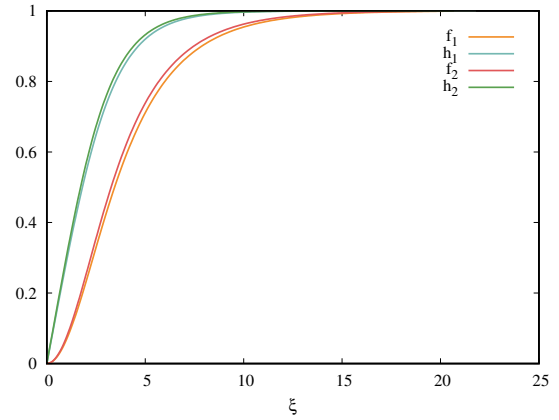
(a) Profile functions with  $a = 1.1$



(b) Profile functions with  $a = 1.3$



(c) Profile functions with  $a = 1.5$



(d) Profile functions with  $a = 1.9$

FIG. 3:  $m_{H^\pm}(v_2) = m_A(v_2) = 350$  GeV,  $m_H(v_2) = 160$  GeV.

In Fig.3, the blue lines approach the green lines, the red lines go to the orange lines, as  $a$  increases. The blue and green lines represent the bubbles of gauge fields, the orange and red lines represent the bubbles of Higgs fields, corresponding to the two phases.

When the phase transition occurs,  $v_2$  is broken before  $v_1$ . The blue and red lines (corresponding to the bubbles associated with  $v_2$ ) approach 1 faster or earlier than the green and orange lines (corresponding to the bubbles associated with  $v_1$ ).

In other words, the process of forming bubble nucleations, to give the masses of particles, from massless one: the first they form a bubble nucleation corresponding to  $v_2$  first, then form a bubble nucleation corresponding to  $v_1$  so the initial particles form a pair of bubble nucleation. But these two nucleations can form at the same time when  $a = 2$ , we can name this pair as a twin bubble nucleation.

And the sphaleron energy as the fifth column in Table III. According to Appendix A,  $a$  and the sphaleron energy both increases. The total energy value of these two phase transitions is in the range of 10 to 15 TeV.

## B. Gravitational waves

The formulas to calculate the gravitational wave energy density (GWED) will be systematized as a setting for the calculation process. There are three processes in the production of GWs with a first-order EWPT: the bubble wall collisions (Coll), sound waves (SW) and Magnetohydrodynamic (MHD) turbulence [94]. Usually they are added linearly to calculate the gravitational wave energy density [94]:

$$h^2\Omega_{GW} = h^2\Omega_{Coll} + h^2\Omega_{sw} + h^2\Omega_{tur}. \quad (15)$$

The GWED of SW depends on  $\alpha$  and  $\beta/H^*$  [94, 95]:

$$h^2\Omega_{sw}(f) \simeq 2.65 \times 10^{-6} v_b k_w^2 \left[ \frac{H_*}{\beta} \right] \left[ \frac{\alpha}{1+\alpha} \right]^2 \left[ \frac{100}{g_*} \right]^{\frac{1}{3}} S_{sw}(f), \quad (16)$$

where

$$S_{sw}(f) = (f/f_{sw})^3 \left( \frac{7}{4 + 3(f/f_{peak.sw})^2} \right)^{7/2}, \quad (17)$$

and at the temperature  $T_*$ , the nucleation temperature [94], the peak frequency estimated as follows

$$f_{peak.sw} = 1.9 \times 10^{-2} mHz \times \frac{1}{v_b} \frac{\beta}{H^*} \frac{T_*}{100} \left( \frac{g_*}{100} \right)^{1/6}. \quad (18)$$

The bubble wall velocity is defined via  $\alpha$  [94]:

$$v_{bn} = \frac{\frac{1}{\sqrt{3}} + \sqrt{\alpha^2 + 2\frac{\alpha}{3}}}{1 + \alpha}. \quad (19)$$

From the value of  $\alpha$  in Table III and Appendix A,  $v_{bn}$  is around  $0.75 \sim 1$ , that is, it can be compared to 1, or it has size 1. Therefore, the generation of gravitational waves has only two components: the sound wave and turbulence [94, 96–101].

GWs from turbulence,

$$h^2 \Omega_{tur}(f) \simeq 3.35 \times 10^{-4} \left( \frac{H^*}{\beta} \right) v_b \left( \frac{k_t \alpha}{1 + \alpha} \right)^{\frac{3}{2}} \left( \frac{100}{g^*} \right)^{1/3} S_{tur}(f), \quad (20)$$

in which

$$S_{tur}(f) = \frac{(f/f_{peak.tur})^3}{(1 + (f/f_{peak.tur}))^{11/3} (1 + 8\pi f/h^*)}, \quad (21)$$

and at  $T_*$ , Eq. (21) reads

$$\begin{aligned} h_* &= 16.5 \times 10^{-3} mHz \times \frac{T_*}{100} \left( \frac{g_*}{100} \right)^{1/6}, \\ f_{peak.tur} &= 2.7 \times 10^{-2} mHz \times \frac{1}{v_b} \frac{\beta}{H^*} \frac{T_*}{100} \left( \frac{g_*}{100} \right)^{1/6}. \end{aligned} \quad (22)$$

One can estimate [94] that

$$k_t = (0.05 - 0.1) \times k_w; \quad k_w = \alpha [0.73 + 0.083\sqrt{\alpha} + \alpha]^{-1} \quad \text{when} \quad v_{bn} \sim 1. \quad (23)$$

The next, in Table IV, the contribution of the Higgs field component to the total Sphaleron energy is on average about 45% and by using a possible approximation [102], because when calculating GW we only consider the effective potential and scalar field component [94, 95],

$$\frac{\beta}{H^*} \approx \left[ T \frac{d \left( 0.45 \frac{E_{sph,b}^T}{T} \right)}{dT} \right]_{T=T_C}, \quad (24)$$

in which  $\frac{\beta}{H^*}$  is a dimensionless quantity and is calculated using the sphaleron energy and the potential energy. Additionally, in Ref. [104], at  $T_* = T_c$ ,  $H^*$  is estimated as

$$H^* = 4.5 \times 10^{-22} \left[ \frac{T_c}{MeV} \right]^2 \text{ MeV} \left[ \frac{g_*}{10.75} \right]^2; \quad g^* = 106.75. \quad (25)$$



	$E_{Higgs,b}^T/E_{sph,b}^T(\%)$			
a	$(m_{H^\pm}(v_2), m_H(v_2))$ (600, 300)[GeV]	$(m_{H^\pm}(v_2), m_H(v_2))$ (500, 250)[GeV]	$(m_{H^\pm}(v_2), m_H(v_2))$ (350, 160)[GeV]	$(m_{H^\pm}(v_2), m_H(v_2))$ (300, 150)[GeV]
1.1	43.7192	44.1598	45.7986	46.6429
1.2	43.6772	44.0209	45.5623	46.4284
1.3	43.6652	43.9105	45.3493	46.2181
1.4	43.6798	43.8245	45.1576	46.0172
1.5	43.7177	43.7595	44.9851	45.8281
1.6	43.7761	43.7129	44.8297	45.6517
1.7	43.8521	43.6829	44.6897	45.488
1.8	43.9425	43.6677	44.5634	45.3363
1.9	44.0446	43.6661	44.4493	45.1959
2	44.1555	43.677	44.3465	45.0659

TABLE IV: The ratio between the Higgs component and the total sphaleron energy.

In Table IV,  $E_{Higgs,b}^T$  is the components containing only the function  $h_b(\xi)$  in Eq.11, in most cases  $E_{Higgs,b}^T/E_{sph,b}^T$  decreases as  $a$  increases. It ranges from 43.67% to 46.64%. So the average of this ratio is around 45%. We therefore approximate it as Eq.24. We also find that this ratio holds for most models because the contribution of the effective potential component to sphaleron is quite small. Indeed, this ratio in the THD model is exactly the same as the result in Ref. [102].

The last parameter is  $\alpha$  [105–107], summarized as the below formulas:

$$\alpha = \frac{\epsilon}{\rho_{rad}^*}, \rho_{rad}^* = g^* \pi^2 \frac{T_c^4}{30} = 106.75 \pi^2 \frac{T_c^4}{30}, \quad (26)$$

$$\epsilon = \left( V_{eff}(v(T), T) - T \frac{d}{dT} V_{eff}(v(T), T) \right)_{T=T_C}. \quad (27)$$

$\alpha$  depends almost entirely on the effective potential. Therefore, in models, for a one-loop effective potential,  $\alpha$  can be estimated under a value of  $S$  and GW can be calculated at  $T_c$ .

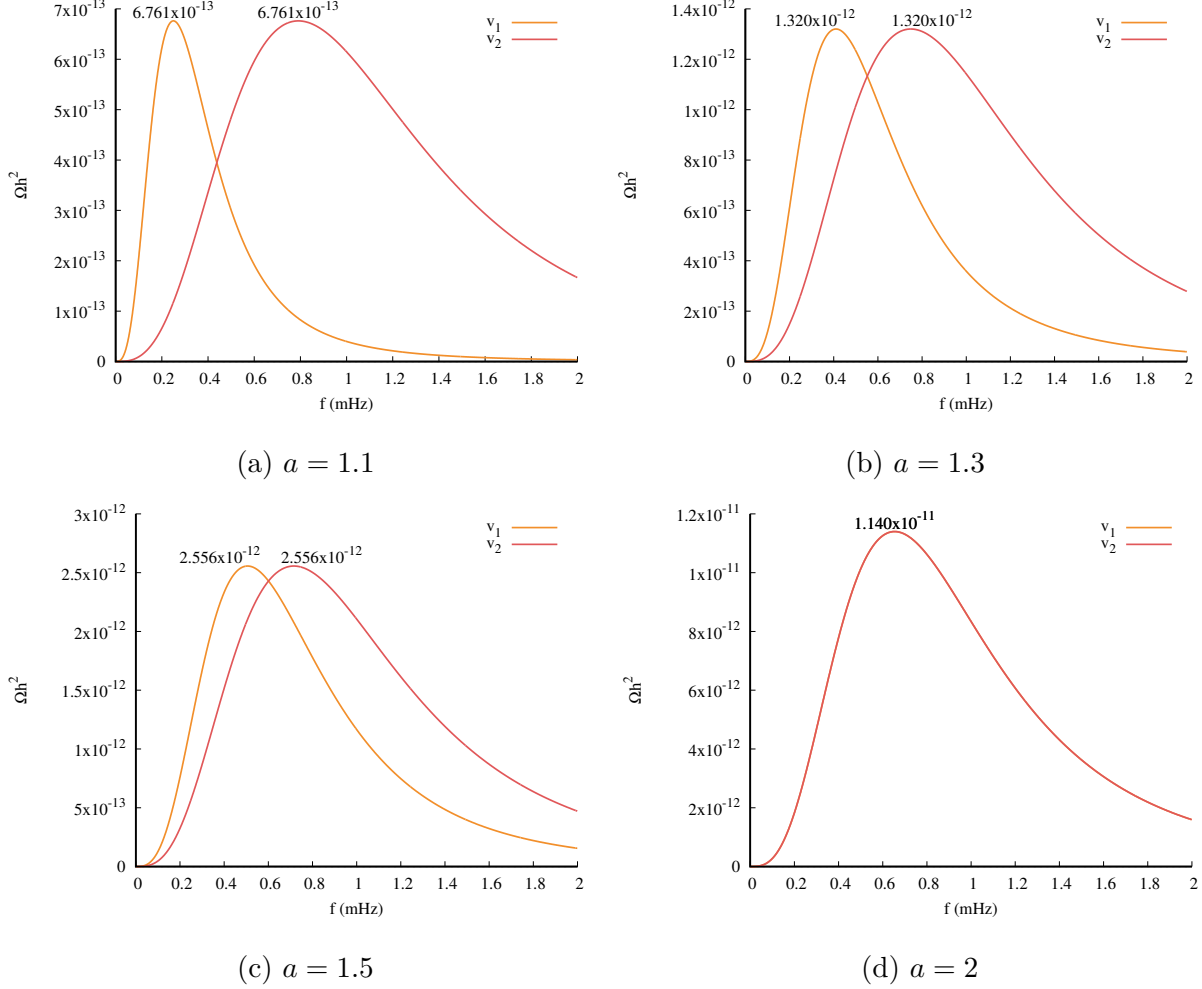


FIG. 4: Gravitational wave energy density at  $T_* = T_C$ . The blue line corresponds to  $v_2$ , the purple line corresponds to  $v_1$ .  $m_{H^\pm}(v_2) = m_A(v_2) = 600$  GeV,  $m_H(v_2) = 300$  GeV.

The two lines in each sub-figure in Fig.4 go closer to each other as  $a$  increases. This is also consistent with the previous observations about the two EWPT stages.

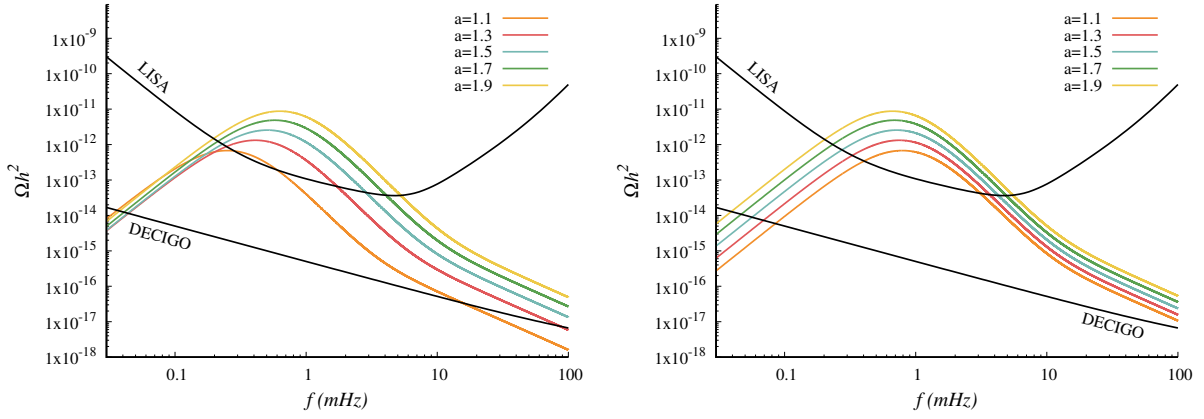
From the numerical results in Table III and Appendix A, the gravitational wave energy density of two phase transitions are equal at  $f = f_{peak}$  at  $T_c$ . This is shown visually in Fig. 4. Because  $a$  does not affect the phase transition strength of the two stages (i.e. the phase transition strength of the two stages is equal for one value of  $a$ ).  $\Omega h^2$  ranges widely, from  $10^{-14}$  to  $10^{-11}$ . As  $a$  increases,  $\Omega h^2$  increases sharply.

The gravitational wave detection frequency is solved in the range below a few mHz. At such low frequencies there is currently no experimental data. However, future detectors may be able to detect gravitational energy densities in the small frequency range as summarized

in Table V. The LISA and DECIGO detectors can pick up the gravitational wave signal generated by the EWPT process in the 2HDM- $S_3$  model as shown in Figs. 5, 6.

$f[\text{mHz}]$	$\Omega h^2$	Kind	Refs.
$0.02 - 0.12$	$2 \times 10^{-12} - 10^{-10}$	LISA	Refs.[108–110]
$0.01 - 0.12$	$5 \times 10^{-15} - 8 \times 10^{-14}$	DECIGO	Refs.[108–110]
$0 - 0.2$	Not yet	BBO	Refs.[108–110]

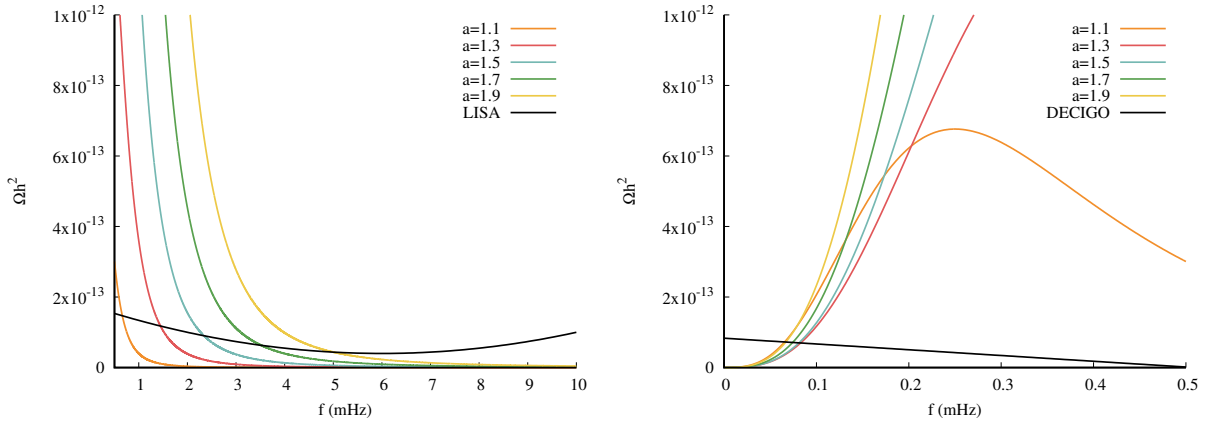
TABLE V: Sensitivity of proposed GW.



(a)  $\Omega h^2$  of the phase transition  $v_1$  [108].

(b)  $\Omega h^2$  of the phase transition  $v_2$  [108].

FIG. 5:  $\Omega h^2$  with  $m_{H^\pm}(v_2) = m_A(v_2) = 600$  GeV,  $m_H(v_2) = 300$  GeV.



(a) Comparison with LISA [108].

(b) Comparison with DECIGO [108].

FIG. 6:  $\Omega h^2$  of the phase transition  $v_1$ .  $m_{H^\pm}(v_2) = m_A(v_2) = 600$  GeV,  $m_H(v_2) = 300$  GeV.

According to Fig. 6, when  $f \leq 1$  mHz the gravitational wave results are consistent with DECIGO but when  $f \sim$  a few mHz, LISA gives better results.

#### IV. CONCLUSION AND OUTLOOKS

$a$	$v_{b0}$ [GeV]	$v_c$ [GeV]	$E_{b0}$ [GeV]	$E_{sph,b}^{T_c}$ [GeV]	$E_{sph,b}^{T_c}/v_c$	$E_{b0}/v_{b0}$	Difference
1.3	$v_{20} = 215.592$	$v_2=153.12$	7902.28	7365.48	48.10	36.65	24%
	$v_{10} = 118.656$	$v_1=83.8672$	4302.69	4034.24	48.10	36.26	
1.5	$v_{20} = 200.96$	$v_2=151.2$	7311.87	6988.23	46.22	36.38	21%
	$v_{10} = 142.026$	$v_1=106.914$	5172.53	4941.43	46.22	36.42	
1.7	$v_{20} = 188.665$	$v_2=149.173$	6826.74	6679.16	44.77	36.18	19%
	$v_{10} = 157.979$	$v_1=124.807$	5707.53	5588.19	44.77	36.13	

TABLE VI:  $m_{H^\pm}(v_2) = m_A(v_2) = 350$  GeV,  $m_H(v_2) = 160$  GeV.

According to the data tables, at the same value of  $a$ , the ratio  $E_{sph,b}^T/v_b$  is always equal. By the linear scaling law of sphaleron energy [43–45],  $E_{sph,b}^T/v_b = E_{b0}/v_{b0} = \text{const}$  ( $E_{b0}$  is the sphaleron energy at  $T = 0$ , Eq. (13) calculated by replacing the effective potential at temperature  $T$  with one at 0), the evolution (increase or decrease of sphaleron energy) in the two phase transitions is the same. However,  $a$  and this progression increase proportionally.

Additionally to test the scaling law (however, this was initially only an approximation to solve the Sphaleron energy problem [44, 45]). We estimate some cases like Table VI,  $E_{sph,b}^T/v_b$  and  $E_{b0}/v_{b0}$  differ by no more than 24%. Thus the results are not very compatible with the scaling law or this law is only true in a non-zero temperature range but is not true in the temperature range from 0 to  $T_c$ . For some other cases the calculation also breaks this law as in Ref.[111]. Because there are many triggers outside SM and energy scales other than SM. Furthermore, the solutions  $h(\xi)$  and  $f(\xi)$  in Eqs. (13) will approach 1 very slowly at 0, leading to  $E_0$  no longer holding the Scaling law. Furthermore, since  $v_{eff}(T)$  is only used for non-zero temperatures, that is,  $V_{eff}(0) \neq \lim_{T \rightarrow 0} v_{eff}(T)$ .

The total sphaleron energy of two phase transitions is about 10 – 13 TeV in this model. The value differs by about 1 – 5 TeV from the SM. We also need to check the decoupling

condition of sphaleron energy [112–114] as the following formula,

$$\frac{E_{sph,b}^T}{T} - 7\ln\left(\frac{v(T)}{T}\right) + \ln\left(\frac{T}{100\text{GeV}}\right) > (35.9 - 42.8). \quad (28)$$

Based on the data tables in Appendix A, the  $\frac{E_{sph,b}^T}{T}$  ratio is always greater than 50;  $v_c$  is not much bigger than  $T_c$  and almost  $T_c$  are larger than 100 GeV so  $[-7\ln(v_c/T_c) + \ln(T/100)]$  has a negative value but not less than  $-5$ . Thus the sphaleron energy always satisfies the decoupling condition in Eq. (28). Also, the nucleation temperature  $T_N$  is not much larger than  $T_C$ , the supercooling process is small. In other words, the onset of phase transition is not so slow. However, the smaller  $a$  is, the larger the gap between two phases is, the longer the EWPT is, another supercooling process in this model.

$\beta/H^*$  is actually quite difficult to calculate, it is estimated by us from the different contributions to the sphaleron energy. Based on numerical calculations, the contribution of gauge field component to this energy is 55% so having an approximation as Eq.(24). In general an approximation,  $\frac{\beta}{H^*} \approx T \frac{d}{dT} \left( \gamma \cdot \frac{E_{sph,b}^T}{T} \right)$  can be choosed for other models;  $\gamma$  depends on the contributions of components.

In the future, with new experimental data from the LHC, simply confirming the signals of particles beyond SM or sphaleron, it will indirectly confirm the Baryogenesis scenario.

Thus the baryogenesis scenario in the 2HDM- $S_3$  model is fully calculated. One assertion is that this model has enough triggers to generate a first order electroweak phase transition, with sphaleron energies around the mid-range value of about 10 TeV which are checked by theoretical conditions and GW energies are compared with experimental possibilities. Additionally, the prospects for GW, which can be used for further reference, found in Ref.[115].

Our future work follows the results, calculating CP violation, searching and connecting the strength of EWPT, sphalerons or gravitational waves with experimental data. Furthermore, we will extend these results in combination with some nonstandard cosmology scenarios and dark matter as in Refs.[116, 117].

## ACKNOWLEDGMENTS

This research is funded by Vietnam National Foundation for Science and Technology Development (NAFOSTED) under grant number 103.01-2023.16.

## Appendix A: Table of data

a	$v_c$ [GeV]	$T_c$ [GeV]	$S$	$E$ [GeV]	$\alpha$	$\frac{\beta}{H^*}$	$\Omega h^2(f_{peak}) \times 10^{-15}$
1.1	$v_2=128.327$	166.643	0.770071	7621.73	0.0101885	20.5816	2.40066
	$v_1=40.5805$	52.697	0.770071	2410.2	0.0101885	20.5816	2.40066
1.2	$v_2=128.655$	159.876	0.804718	7346.95	0.0114752	20.6793	3.81175
	$v_1=57.5363$	71.4987	0.804717	3285.66	0.0114752	20.6793	3.81173
1.3	$v_2=128.713$	153.922	0.836219	7109.38	0.0127468	20.7847	5.727
	$v_1=70.4988$	84.3067	0.836219	3893.97	0.0127468	20.7847	5.72701
1.4	$v_2=128.568$	148.628	0.86503	6901.35	0.0139997	20.8951	8.22445
	$v_1=81.3135$	94.0008	0.86503	4364.8	0.0139997	20.8951	8.22446
1.5	$v_2=128.272$	143.878	0.891532	6717.06	0.0152319	21.0086	11.3772
	$v_1=90.7021$	101.737	0.891532	4749.68	0.0152318	21.0086	11.3772
1.6	$v_2=127.864$	139.583	0.916043	6552.06	0.016442	21.1231	15.2531
	$v_1=99.043$	108.12	0.916043	5075.2	0.016442	21.1231	15.2531
1.7	$v_2=127.373$	135.672	0.93883	6402.96	0.0176299	21.2375	19.9147
	$v_1=106.568$	113.511	0.93883	5357.1	0.0176299	21.2375	19.9147
1.8	$v_2=126.821$	132.089	0.960119	6267.14	0.0187957	21.3509	25.4201
	$v_1=113.432$	118.144	0.960119	5605.5	0.0187957	21.3509	25.4201
1.9	$v_2=126.226$	128.789	0.980101	6142.58	0.01994	21.4628	31.8231
	$v_1=119.748$	122.18	0.980101	5827.37	0.01994	21.4628	31.8231
2	$v_2=125.602$	125.735	0.998942	6027.68	0.0210635	21.5728	39.1746
	$v_1=125.602$	125.735	0.998942	6027.68	0.0210635	21.5728	39.1746

TABLE VII: Results in case  $m_{H^\pm}(v_2) = m_A(v_2) = 300$  GeV,  $m_H(v_2) = 150$  GeV.

a	$v_c$ [GeV]	$T_c$ [GeV]	$S$	$E$ [GeV]	$\alpha$	$\frac{\beta}{H_*}$	$\Omega h^2(f_{peak}) \times 10^{-13}$
1.1	$v_2=198.272$	171.699	1.15477	8634.25	0.0319842	22.6293	1.87205
	$v_1=62.6992$	54.2959	1.15477	2730.39	0.0319842	22.6293	1.87205
1.2	$v_2=195.78$	164.759	1.18829	8377.36	0.0346998	22.8808	2.52906
	$v_1=87.5557$	73.6823	1.18829	3746.47	0.0346998	22.8808	2.52906
1.3	$v_2=193.537$	158.617	1.22015	8150.04	0.037412	23.1218	3.33497
	$v_1=106.004$	86.8783	1.22015	4463.96	0.037412	23.1218	3.33497
1.4	$v_2=191.544$	153.149	1.25071	7947.12	0.0401542	23.3511	4.32144
	$v_1=121.143$	96.86	1.25071	5026.2	0.0401542	23.3511	4.32144
1.5	$v_2=189.799$	148.262	1.28016	7764.6	0.0429607	23.5669	5.53165
	$v_1=134.208$	104.837	1.28016	5490.4	0.0429607	23.5669	5.53165
1.6	$v_2=188.289$	143.888	1.30859	7599.4	0.0458661	23.7667	7.02374
	$v_1=145.848$	111.455	1.30859	5886.47	0.0458661	23.7667	7.02374
1.7	$v_2=186.999$	139.975	1.33595	7449.03	0.0489043	23.9476	8.87484
	$v_1=156.455$	117.111	1.33595	6232.31	0.0489043	23.9476	8.87484
1.8	$v_2=185.909$	136.483	1.36213	7311.46	0.0521068	24.1066	11.1852
	$v_1=166.282$	122.074	1.36213	6539.57	0.0521068	24.1066	11.1852
1.9	$v_2=184.994$	133.381	1.38696	7184.98	0.0555005	24.2407	14.0822
	$v_1=175.5$	126.536	1.38696	6816.27	0.0555005	24.2407	14.0822
2	$v_2=184.227$	130.638	1.41021	7068.15	0.0591052	24.3471	17.7223
	$v_1=184.227$	130.638	1.41021	7068.15	0.0591052	24.3471	17.7223

TABLE VIII: Results in case  $m_{H^\pm}(v_2) = m_A(v_2) = 500$  GeV,  $m_H(v_2) = 250$  GeV.

a	$v_c$ [GeV]	$T_c$ [GeV]	$S$	$E$ [GeV]	$\alpha$	$\frac{\beta}{H_*}$	$\Omega h^2(f_{peak}) \times 10^{-12}$
1.1	$v_2=226.219$	173.466	1.30411	9149.73	0.0453932	23.7359	0.676314
	$v_1=71.5367$	54.8549	1.30411	2893.4	0.0453932	23.7359	0.676314
1.2	$v_2=224.01$	166.748	1.34341	8891.16	0.0497831	23.9945	0.94705
	$v_1=100.18$	74.5718	1.34341	3976.25	0.0497831	23.9945	0.94705
1.3	$v_2=222.28$	161.054	1.38016	8663.24	0.0545297	24.2059	1.32034
	$v_1=121.748$	88.213	1.38016	4745.05	0.0545297	24.2059	1.32034
1.4	$v_2=220.939$	156.277	1.41376	8460.32	0.0597024	24.3614	1.83858
	$v_1=139.734$	98.8385	1.41376	5350.77	0.0597024	24.3614	1.83858
1.5	$v_2=219.885$	152.323	1.44354	8277.83	0.0653321	24.4547	2.55674
	$v_1=155.482$	107.709	1.44354	5853.31	0.0653321	24.4547	2.55674
1.6	$v_2=219.015$	149.102	1.4689	8112.05	0.0713998	24.4827	3.54026
	$v_1=169.648$	115.494	1.4689	6283.56	0.0713998	24.4827	3.54026
1.7	$v_2=218.235$	146.522	1.48943	7959.9	0.0778348	24.4464	4.85909
	$v_1=182.588$	122.589	1.48943	6659.73	0.0778348	24.4464	4.85909
1.8	$v_2=217.466$	144.494	1.50501	7818.9	0.0845259	24.3505	6.57865
	$v_1=194.508$	129.24	1.50501	6993.43	0.0845259	24.3505	6.57865
1.9	$v_2=216.653$	142.93	1.5158	7687.09	0.0913395	24.2019	8.74961
	$v_1=205.535$	135.596	1.5158	7292.61	0.0913395	24.2019	8.74961
2	$v_2=215.759$	141.75	1.52211	7562.95	0.0981397	24.0094	11.3997
	$v_1=215.759$	141.75	1.52211	7562.95	0.0981397	24.0094	11.3997

TABLE IX: Results in case  $m_{H^\pm}(v_2) = m_A(v_2) = 600$  GeV,  $m_H(v_2) = 300$  GeV.



- 
- [1] M. I. Dine, R. G. Leigh, P. Huet, A. Linde, and D. Linde, Phys. Rev. D **46**, 550 (1992).
  - [2] K. Kajantie, M. Laine, K. Rummukainen, and M. Shaposhnikov, Phys. Rev. Lett. **77**, 2887 (1996).
  - [3] F. Csikor, Z. Fodor, and J. Heitger, Phys. Rev. Lett. **82**, 21 (1999).
  - [4] J. Grant and M. Hindmarsh, Phys. Rev. D **64**, 016002 (2001).
  - [5] M. D’Onofrio, K. Rummukainen and A. Tranberg, J. High Energy Phys. **08** (2012) 123.
  - [6] M. D’Onofrio, K. Rummukainen, and A. Tranberg, Phys. Rev. Lett. **113**, 141602 (2014).
  - [7] Vo Quoc Phong, Vo Thanh Van, and Hoang Ngoc Long, Phys. Rev. D **88**, 096009 (2013).
  - [8] A. Menon, D. E. Morrissey, and C. E. M. Wagner, Phys. Rev. D **70**, 035005 (2004).
  - [9] S. W. Ham, S. K. Oh, C. M. Kim, E. J. Yoo, and D. Son, Phys. Rev. D **70**, 075001 (2004).
  - [10] M. Bastero-Gil, C. Hugonie, S. F. King, D. P. Roy, and S. Vempati, Phys. Lett. B **489**, 359 (2000).
  - [11] A. Menon, D. E. Morrissey, and C. E. M. Wagner, Phys. Rev. D **70**, 035005 (2004).
  - [12] J. M. Cline, G. Laporte, H. Yamashita and S. Kraml, J. High Energy Phys. **0907** (2009) 040.
  - [13] A. Azatov and M. Vanvlasselaer, J. High Energy Phys. **09** (2020) 085.
  - [14] G. C. Dorsch, S. J. Huber, and J. M. No, J. High Energy Phys. **10** (2013) 029.
  - [15] S. W. Ham, S-A Shim, and S. K. Oh, Phys. Rev. D **81**, 055015 (2010).
  - [16] D. Borah and J. M. Cline, Phys. Rev. D **86**, 055001 (2012).
  - [17] A. Ahriche and S. Nasri, Phys. Rev. D **85**, 093007 (2012).
  - [18] S. Das, P. J. Fox, A. Kumar, and N. Weiner, J. High Energy Phys. **1011** (2010) 108.
  - [19] D. Chung and A. J. Long, Phys. Rev. D **84**, 103513 (2011).
  - [20] M. Carena, N. R. Shaha, and C. E. M. Wagner, Phys. Rev. D **85**, 036003 (2012).
  - [21] V. Q. Phong, H. N. Long, V. T. Van, and N. C. Thanh, Phys. Rev. D **90**, 085019 (2014).
  - [22] J. Sá Borges and R. O.Ramos, Eur. Phys. J. C **76**, 344 (2016).
  - [23] V. Q. Phong, H. N. Long, V. T. Van, and L. H. Minh, Eur. Phys. J. C **75**, 342 (2015).
  - [24] J. R. Espinosa, T. Konstandin, and F. Riva, Nucl. Phys. **B854**, 592 (2012).
  - [25] D. J. H. Chung and A. J. Long, Phys. Rev. D **81**, 123531 (2010).
  - [26] G. Barenboim and N. Rius, Phys. Rev. D **58**, 065010 (1998).

- [27] S. Profumo, M. J. Ramsey-Musolf, and G. Shaughnessy, J. High Energy Phys. **0708** (2007) 010.
- [28] S. Profumo, M. J. Ramsey-Musolf, C. L. Wainwright, and P. Winslow, Phys. Rev. D **91**, 035018 (2015).
- [29] D. Curtin, P. Meade, and C-T. Yu, J. High Energy Phys. **11** (2014) 127.
- [30] M. Jiang, L. Bian, W. Huang, and J. Shu, Phys. Rev. D **93**, 065032 (2016).
- [31] M. Carena, G. Nardini, M. Quiros, and C. E.M. Wagner, Nucl. Phys. **B812**, 243 (2009).
- [32] A. Katz, M. Perelstein, M. J. Ramsey-Musolf, and P. Winslow, Phys. Rev. D **92**, 095019 (2015).
- [33] J. Kozaczuk, S. Profumo, L. S. Haskins, C. L. Wainwright, J. High Energy Phys. **1501** (2015) 144.
- [34] H. H. Patel and M. J. Ramsey-Musolf, Phys. Rev. D. **88**, 035013 (2013).
- [35] N. Blinov, J. Kozaczuk, D. E. Morrissey, and C. Tamarit, Phys. Rev. D **92**, 035012 (2015).
- [36] S. Inoue, G. Ovanessian, and M. J. Ramsey-Musolf, Phys. Rev. D **93**, 015013 (2016).
- [37] H. H. Patel and M. J. Ramsey-Musolf, J. High Energy Phys. **1107** (2011) 029.
- [38] G. W. Anderson and L. J. Hall, Phys. Rev. D **45**, 2685 (1992).
- [39] H. H. Patel, M.J. Ramsey-Musolf, M. Garny and T. Konstandin, J. High Energy Phys. **1207** (2012) 189.
- [40] J. De Vries, M. Postma, and J. van de Vis, J. High Energy Phys. **1904** (2019) 024.
- [41] J. de Vries, M. Postma, J. van de Vis , G. White, J. High Energy Phys. **1801** (2018) 089.
- [42] C. Balazs, G. White, and J. Yue, J. High Energy Phys. **1703** (2017) 030.
- [43] Yves Brihaye and Jutta Kunz Phys. Rev. D **48**, 3884 (1993).
- [44] Sylvie Braibant, Yves Brihaye, Jutta Kunz, Int.J.Mod.Phys. A **8** (1993) 5563-5574.
- [45] Ruiyu Zhou, Ligong Bian, and Huai-Ke Guo, Phys. Rev. D **101**, 091903(R) (2020).
- [46] A. Ahriche and S. Nasri, J. Cosmol. Astropart. Phys. **07** (2013) 035.
- [47] A. Ahriche, G. Faisel, S. Y. Ho, S. Nasri and J. Tandean, Phys. Rev. D **92**, 035020 (2015).
- [48] A. Ahriche, K. L. McDonald and S. Nasri, Phys. Rev. D **92**, 095020 (2015).
- [49] A. Ahriche, S. M. Boucenna and S. Nasri, Phys. Rev. D **93**, 075036 (2016).
- [50] A. Ahriche, K. Hashino, S. Kanemura and S. Nasri, Phys. Lett. B **789**, 119 (2019).
- [51] C. Grojean, G. Servant, and J. D. Wells, Phys. Rev. D **71** 036001 (2005).
- [52] C. Delaunay, C. Grojean, J. D. Wells, J. High Energy Phys. **0804** (2008) 029.

- [53] A. Kusenko, L. Pearce, and L. Yang, Phys. Rev. Lett. **114**, 061302 (2015).
- [54] Vo Quoc Phong, Dam Quang Nam, International Journal of Modern Physics A, 2350159 (2023).
- [55] A. D. Sakharov, JETP Lett. **5**, 24 (1967).
- [56] Vo Quoc Phong, Phan Hong Khiem, Ngo Phuc Duc Loc, and Hoang Ngoc Long, Phys. Rev. D **101**, 116010 (2020).
- [57] A. Braconi, Mu-Chun Chen, and G. Gaswint, Phys. Rev. D **100**, 015032 (2019).
- [58] I. Baldes, T. Konstandin, and G. Servant, Phys. Lett. B **786**, 373 (2018).
- [59] V. Q. Phong, N. C. Thao, and H. N. Long, Phys. Rev. D **97**, 115008 (2018).
- [60] Djuna Croon, Oliver Gould, Philipp Schicho, Tuomas V. I. Tenkanen, Graham White, JHEP **04** (2021) 055.
- [61] Vo Quoc Phong, N. T. Tuong, N. C. Thao, and H. N. Long, Phys. Rev. D **99**, 015035 (2019).
- [62] Vo Quoc Phong and Nguyen Minh Anh, Int. J. Mod. Phys. A **34**, 1950073 (2019).
- [63] M. Aoki, T. Komatsu, and H. Shibuya, Prog. Theor. Exp. Phys. **2022**, 063B05.
- [64] D. Gonçalves, A. Kaladharan, and Y. Wu, Phys. Rev. D **105**, 095041 (2022).
- [65] Vo Quoc Phong, Nguyen Minh Anh, Hoang Ngoc Long, Phys. Rev. D **107**, 035020 (2023).
- [66] D. Cogollo and J. P. Silva, Phys. Rev. D **93**, 095024 (2016).
- [67] D. Das, U. K. Dey, and Palash B. Pal, Phys. Rev. D **96**, 031701 (2017).
- [68] D. Das and U. K. Dey, Phys. Rev. D **89**, 095025 (2014); **91**, 039905(E) (2015).
- [69] D. Das, U. K. Dey and Palash B. Pal, Phys. Lett. B **753**, 315 (2016).
- [70] A. Braconi, Mu-Chun Chen, Geoffrey Gaswint, Phys. Rev. D **100**, 015032 (2019).
- [71] A. Arbey, F. Mahmoudi, O. Stal, and T. Stefaniak, Eur. Phys. J. C **78**, 182 (2018).
- [72] W. Mader, Jae-hyeon Park, G. M. Pruna, D. Stöckinger, and A. Straessner, J. High Energy Phys. **1209** (2012) 125.
- [73] V. Khachatryan *et al*, Phys. Lett. B **758**, 296 (2016).
- [74] P. Basler, M. Mühlleitner, and J. Wittbrodt, J. High Energy Phys. **03** (2018) 061.
- [75] J. R. Espinosa, T. Konstandin, J. M. No and M. Quiros, Phys. Rev. D **78**, 123528 (2008).
- [76] D. Comelli and J.R. Espinosa, Phys.Rev. D **55**, 6253 (1997).
- [77] G. C. Dorsch, S. J. Huber, and J. M. No, J. High Energy Phys. **10** (2013) 029.
- [78] N. Blinov, S. Profumo, and T. Stefaniak, J. Cosmol. Astropart. Phys. **07** (2015) 028.

- [79] J. O. Andersen, T. Gorda, A. Helset, L. Niemi, T. V. I. Tenkanen, A. Tranberg, A. Vuorinen, and D. J. Weir, *Phys. Rev. Lett.* **121**, 191802 (2018).
- [80] G. C. Dorsch, S. J. Huber, K. Mimasu, and J.M. Nob, *J. High Energy Phys.* **02** (2017) 121.
- [81] K. Enomoto, S. Kanemura, and Y. Mura, *J. High Energy Phys.* **01** (2022) 104.
- [82] K. Kainulainen, V. Keus, L. Niemi, K. Rummukainen, T. V.I. Tenkanen, and V. Vaskonen, *J. High Energy Phys.* **06** (2019) 075.
- [83] P. Basler, M. Krause, M. Mühlleitner, J. Wittbrodt, and A. Wlotzka, *J. High Energy Phys.* **12** (2017) 086.
- [84] J. Bernon, L. Biana, and Y. Jiang, *J. High Energy Phys.* **05** (2018) 151.
- [85] Shinya Kanemura, Masanori Tanaka, *Phys. Rev. D.* **106**, 035012 (2022).
- [86] Thomas Biekötter, Sven Heinemeyer, José Miguel No, María Olalla Olea-Romacho, Georg Weiglein, *JCAP* **03**,031 (2023).
- [87] S. Davidson and H. E. Haber, *Phys. Rev. D* **72**, 035004 (2005); **72**, 099902(E) (2005).
- [88] Wei Su, A. G. Williams, and M. Zhang, *J. High Energy Phys.* **04** (2021) 219.
- [89] R. Zhou and L. Bian, *Phys. Lett. B* **829**, 137105 (2022).
- [90] F. R. Klinkhamer and N. S. Manton, *Phys. Rev. D* **30**, 2212 (1984).
- [91] Xucheng Gan, Andrew J. Long, and Lian-Tao Wang, *Phys. Rev. D* **96**, 115018 (2017).
- [92] Koichi Funakubo and Eibun Senaha, *Phys. Rev. D* **79**, 115024 (2009).
- [93] E. Ma and B. Melic, *Phys. Lett. B* **725**, 402 (2013).
- [94] Chiara Caprini, Mark Hindmarsh, Stephan Huber, Thomas Konstandin, Jonathan Kozaczuk, Germano Nardini, Jose Miguel No, Antoine Petiteau, Pedro Schwaller, Geraldine Servant, David J. Weir, *JCAP* **04**, 001 (2016).
- [95] R. Zhou, L. Bian and H-K Guo, *Phys. Rev. D* **101**, 091903 (2020).
- [96] A. Kosowsky, M. S. Turner, and R. Watkins, *Phys. Rev. D* **45**, 4514 (1992).
- [97] A. Kosowsky, M. S. Turner, and R. Watkins, *Phys. Rev. Lett.* **69**, 2026 (1992).
- [98] A. Kosowsky and M. S. Turner, *Phys. Rev. D* **47**, 4372 (1993).
- [99] S. J. Huber and T. Konstandin, *JCAP* **08099**, 022 (2008).
- [100] R. Jinno and M. Takimoto, *Phys. Rev. D* **95**, 024009 (2017).
- [101] R. Jinno and M. Takimoto, *JCAP* **1901**, 060 (2019).
- [102] Vo Quoc Phong, Nguyen Chi Thao and Hoang Ngoc Long, *Eur. Phys. J. C* **82**, 1005 (2022).
- [103] M. Laine, M. Meyer, G. Nardini, *Nuclear Physics B* **920**, 565-600 (2017).

- [104] A. D. Dolgov, D. Grasso, A. Nicolis, Phys. Rev. D **66**, 103505 (2002).
- [105] L. Leitaο, A. Megevand, A. D. Sanchez, JCAP **10**, 024 (2012).
- [106] M. S Tuner and S. Wilzek, Phy. Rev. **65**, 3080 (1990).
- [107] Christophe Grojean, G. Servant, Phys. Rev. D **75**, 043507 (2007).
- [108] S.V. Demidov, D. S. Gorbunov, D. V. Kirpichnikov, Physics Letters B **779**, 191 (2018).
- [109] Hideaki Kudoh, Atsushi Taruya, Takashi Hiramatsu, and Yoshiaki Himemoto, Phys. Rev. D **73**, 064006 (2006).
- [110] Eric Thrane<sup>1</sup> and Joseph D. Romano, Phys. Rev. D **88**, 124032 (2013).
- [111] Xucheng Gan, Andrew J. Long, and Lian-Tao Wang, Phys. Rev. D **96**, 115018 (2017).
- [112] K. Funakubo and E. Senaha, Phys. Rev. D **79**, 115024 (2009).
- [113] M. Dvornikov and V. B. Semikoz, Phys. Rev. D **87**, 025023 (2013).
- [114] T. M. Gould and I. Z. Rothstein, Phys. Rev. D **48**, 5917 (1993).
- [115] Rishav Roshan, Graham White, Rev. Mod. Phys. **97**, 015001 (2025).
- [116] Ngo Phuc Duc Loc, Int. J. Mod. Phys. A **37**, 2250153 (2022).
- [117] Rouzbeh Allahverdi, Ngo Phuc Duc Loc, Jacek K. Osinski, Phys. Rev. D **107**,123510 (2023).